Yield functions of unsaturated soil

Les fonctions d'écoulement des sols non saturés

D.KARUBE, Associate Professor of Civil Engineering, Kobe University, Kobe, Japan
S.KATO, Technical Assistant of Civil Engineering, Kobe University, Kobe, Japan

SYNOPSIS In recent years attempts to construct constitutive equations of unsaturated soil applying elasto-plastic theory have been proceeding. This paper proposes yield loci based on Cam Clay type energy equation and experimental results. Then equations of plastic strain increments are obtained by use of associate flow rule. Proposed yield loci are examined by existing results of stress probe test on compacted kaolin clay and are revised to a set of combined yield loci. Associated equations of strain increments are also revised:

INTRODUCTION

It was almost thirty years ago Jennings and Burland (1962) and Coleman (1962) emphasized the unique role of suction on mechanical properties of unsaturated soil against Bishop's effective stress equation. Thereafter some studies on relationships among applied stress, suction and strains were made by Barden, Madedor and Sides (1969), Fredlund, Morgenstern and Widger (1978) and other researchers. In recent years attempts to construct constitutive equations of unsaturated soil applying elasto-plastic theory have been proceeding. Karube (1986) proposed a yield function and formulated plastic volumetric strain on p-S plane based on triaxial test results on compacted kaolin clay, in which p denotes total mean principal stress minus pore air pressure and S denotes suction. Katsuyama, Nishiumi and Karube (1987) performed stress probe test and got several yield points in p-S-q space. Alonso, Gens and Hight (1987) introduced a set of yield loci in p-S plane which is more detailed but not quantitative. In addition, they referred a yield surface in p-S-q space standing on above mentioned yield loci. Karube (1987a) proposed a spatial yield function by analogy with Original Cam Clay model. Kogo (1987) defined effective stress using "equivalent pore water pressure" and applied it to generalized Cam Clay type model to obtain constitutive equations .
In this paper, revised yield functions for unsaturated specimen under triaxial compression test are led first, which are examined by the test data and finally equations of strain increments are proposed.

Definition of Symbols

σ_1 and σ_3: maximum and minimum principal stress
u_a and u_w: pore-air and pore-water pressure
$\sigma_m = (\sigma_1 + 2\sigma_3)/3$
$p = \sigma_m - u_a$
$S = u_a - u_w$: suction, S_p: prestress in suction
$f(S)$: effective vertical stress by suction
$\alpha = \dfrac{p}{p+f(S)}$
q_f: deviator stress at failure
$q_f' = q_f + (\Delta v/\Delta\varepsilon)_f$: corrected failure stress
$M = \dfrac{q_f}{p+f(s)}$, $M' = \dfrac{q_f'}{p+f(S)}$, $x' = \dfrac{q'}{M'[p+f(S)]}$
ε_1 and ε_3: strains of which directions coincide with those of σ_1 and σ_3
$\varepsilon = (2/3)(\varepsilon_1 - \varepsilon_3)$: shear strain
$v = \varepsilon_1 + 2\varepsilon_3$: volumetric strain
Δw: change in water content

YIELD SURFACE

Karube, Kato and Katsuyama (1986) performed suction controlled and p-constant triaxial compression test on compacted kaolin clay and obtained experimental failure criterion as ;

$$q_f' = M'[p + f(S)] \tag{1}$$

where $$q_f' = q_f + p\left(\frac{\Delta v}{\Delta\varepsilon}\right)_f \tag{2}$$

and f(S) is a function converting S into p at failure condition.
Combining eq(1) and eq(2), becomes

$$\left(\frac{\Delta v}{\Delta\varepsilon}\right)_f + \frac{q_f}{p} = M'\,\frac{p + f(S)}{p} \tag{3}$$

Meanwhile after Cam Clay model, energy equation of unsaturated soil would be assumed as follows ;

$$p\,dv + q\,d\varepsilon = M'[p+f(S)] + p\,dv^e$$

$$\therefore \frac{dv^p}{d\varepsilon} + \frac{q}{p} = M'\frac{p+f(S)}{p} \tag{4}$$

where $dv^p = dv - dv^e$

In p-constant test Δv is equal to Δv^p , so eq(3) corresponds to eq(4) at failure. Applying associate flow rule to unsaturated soil, strain increment vector crosses to yield locus perpendicularly, i.e.;

$$\frac{dv^p}{d\varepsilon} = -\frac{dq}{dp} \qquad (5)$$

where (dq/dp) denotes gradient of yield locus on S-constant plane.
Combining eq(4) and eq(5),

$$\frac{dq}{dp} - \frac{q}{p} = -M' \frac{p+f(S)}{p}$$

Integrating above equation, equation of yield locus on S-const plane is obtained as follows and shown in Fig.1 ;

$$q = M'p \ln\left(\frac{p_o}{p}\right) + M' f(S)\left(1-\frac{p}{p_o}\right) \qquad (6)$$

or

$$\frac{q}{M' p_o} = -\frac{p}{p_o} \ln\left(\frac{p}{p_o}\right) + \frac{f(S)}{p_o}\left(1-\frac{p}{p_o}\right) \qquad (6a)$$

where p_o is abscissa of yield locus on p-axis.

The stress point p_o is also a point on a yield locus on p-S plane. As to yield locus on p-S plane, both an initial one and subsequent one are assumed. When $f(S_p) > p_p$, in which an initial S_p and p_p are the pre-stress in S and p respectively as shown in Fig.2a, initial yield function is defined as ;

$$S = S_p \qquad (7a)$$

and

$$p = f(S_p)(1-b) + f(S)b \qquad (7b)$$

where b is cotangent of initial yield locus which should be determined by a series of isotropic consolidation tests. The yield locus eq(7a) was proposed by Alonso, et al. (1987). The subsequent yield loci must coincide with contours of plastic volumetric strain, v^p, because it was observed that induced volumetric strain in elasto-plastic region was not influenced by its stress path but defined by current stress state. Referring equation(14) in Karube's paper (1987),

$$v^p = \frac{\lambda-\kappa}{1+e} \ln[p+f(S)] - Q(S) \qquad (8)$$

where Q(S) is arbitrary function of S. Here defining $v^p=0$ on initial yield locus, eq(7), equation of subsequent v^p becomes

$$v^p = \frac{\lambda-\kappa}{1+e} \ln \frac{p+f(S)}{(1+b)\,f(S) + (1-b)\,f(S_p)} \qquad (9)$$

Solving above equation on p, equation of subsequent yield locus is obtained as follows and shown in Fig.2b ;

$$p = [(1+b)\exp(\tfrac{1+e}{\lambda-\kappa} v^p) - 1]\, f(S) + (1-b)\exp(\tfrac{1+e}{\lambda-\kappa} v^p)\, f(S_p) \qquad (9a)$$

When suction is increased from S_p to S_p' corresponding yield locus will be formed as;

$$p = [(1+b)\exp(\tfrac{1+e}{\lambda-\kappa} v^p) - 1]\, f(S) + (1-b)\exp(\tfrac{1+e}{\lambda-\kappa} v^p)\, f(S_p') \qquad (10)$$

The new yield locus, eq(10), is parallel with old one, eq(9a), and situated somewhat backward as shown in Fig.2b. It seems apparently that stress change from point R to R' accompanies no plastic strain increment, however, v^p in eq(10) is measured from another initial locus through point (P_p', S_p'). Therefore total plastic strain from eq(7) to above equation should be the sum of v^p from eq(10) and v^p induced between eq(7) and the equation bellow;

$$p = f(S_p')(1-b) + f(S)b$$

PLASTIC STRAINS

A contour of plastic volumetric strain must coincide with a yield locus because that strain is assumed to be the strain hardening parameter. Therefore plastic volumetric strain on p-q plane (S-constant plane) can be defined equating p_o in eq(6) to p in eq(9). However , eq(6) can not be solved on p_o , so following approximate equation is adapted;

$$\ln[p_o + f(S)] = \alpha\left[x' - \frac{(x')^2}{2}\right] + \frac{(x')^2}{2} + \ln[p+f(S)] \qquad (11)$$

where $\alpha = \dfrac{p}{p+f(S)}$ and $x' = \dfrac{q}{M'[p+f(S)]}$.

Therefore an approximate equation of plastic volumetric strain becomes;

$$v^p = \frac{\lambda-\kappa}{1+e}\left[\alpha\left(x' - \frac{(x')^2}{2}\right) + \frac{(x')^2}{2} + \frac{p+f(S)}{(1+b)\,f(S) + (1-b)\,f(S_p)}\right] \qquad (12)$$

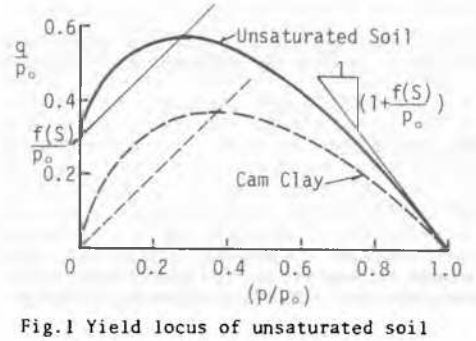

Fig.1 Yield locus of unsaturated soil on S-constant plane

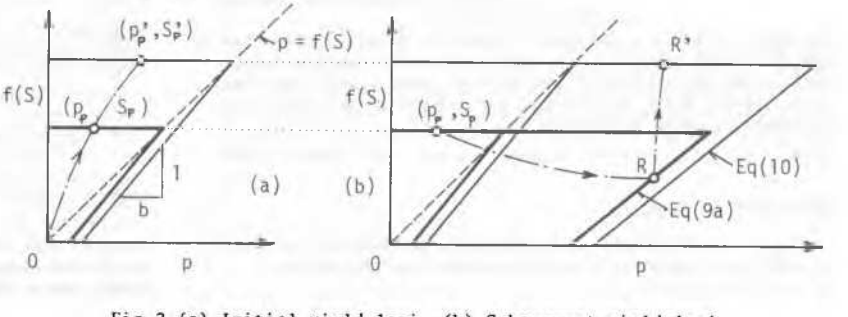

Fig.2 (a) Initial yield loci, (b) Subsequent yield loci

Shear strain increment is obtained using eq(4);

$$d\varepsilon = \frac{\alpha}{M'(1-x')}dv^p$$

$$= \frac{\alpha}{M'(1-x')}\left[\frac{\partial v^p}{\partial p}dp + \frac{\partial v^p}{\partial x'}dx' + \frac{\partial v^p}{\partial f(S)}\frac{df(S)}{dS}dS\right] \quad (13)$$

Substituting dv^p from eq(12) into eq(13), equation of shear strain increment is obtained, however, the function f(S) should be determined. If the loading path is given, eq(13) can be integrated. For instance, the shear strain during p,S-constant test is given by

$$\varepsilon = \frac{\lambda-\kappa}{1+e}\frac{\alpha}{M'}[(\alpha-1)x' - \ln(1-x')] \quad (14)$$

EXAMINATION BY TEST DATA

Katsuyama, et al. (1987) performed four series of triaxial compression test on compacted kaolin clay. Preparation method of specimen was same as Karube (1986) and Karube (1987b).
In the first series (Series 1), specimens traced various consolidation stress paths from point A to C in p-S plane as shown in Fig.3, then those were loaded axially with constant p and S. Specimen No.4 had not experienced any complex consolidation, therefore its whole axial loading path was expected to be in the elasto-plastic zone, and it showed maximum shear and volumetric strain against shear stress, q, as shown in Fig.4. On the other hand, specimen No.5 showed relatively small strains compared with No.4 in spite of monotonic loading from A to C. It seems to indicate that yield locus of No.5 passes somewhat right of point D (see Fig.2b) and the specimen is in elastic zone at beginning of axial compression stage. Specimen No.6 and 7 were pre-stressed in p- and S- direction, respectively and showed small strains in the early stage of axial compression. Specimens in series 2 were loaded along the same path with No.4 in series 1 until shear stress, q, reached 323 kPa (Point I), then were unloaded to 274 kPa (Point J) and finally were loaded to p-direction (No.8), unloaded to (-p)-direction (No.9), unloaded to (-S)-direction (No.10) and unloaded to intermediate direction of -p and -S (No.14) keeping q=274 kPa. The stress paths in final stage are shown in Fig.5. In series 3, specimens (No.8',9',10'and 14') were loaded to 274 kPa (Point J) first, then were loaded or unloaded to the corresponding direction to specimens in series 2. Fig.6 shows the relationships between stress increment ($\Delta\sigma = \Delta p$) and increments of volumetric strain (Δv) in final stage of No.8 and No.8'. It can be recognized from Fig.6a that whole stress path of No.8' is in elasto-plastic zone and on the other hand, No.8 proceeds elastic zone first. Therefore the reason why the ratio; ($\Delta v / \Delta\sigma$), in first part of No.8 is smaller than that of No.8' can be referred to the influence of pre-loading to Point I. Because the ratio ($\Delta v/\Delta\sigma$) of No.8 becomes equal to initial ratio of No.8' at $\Delta\sigma=\Delta p=87$ kPa, the stress point corresponding to the stress increment is regard as the yield point of No.8. Fig.7 shows the similar plots of No.9 and No.9' in which suction was reduced and yield point is estimated as $\Delta\sigma=-\Delta S=-59$ kPa. The yield points of No.10 and 14 were obtained by the same method.
Specimens in series 4 (No.11-13) were loaded to Point I as in series 2, but unloaded to q=196 kPa as shown in Fig.8. Then No.11 was loaded to p-direction by about 100 kPa and finally loaded

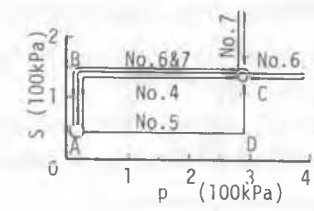

Fig.3 Consolidation paths of series 1

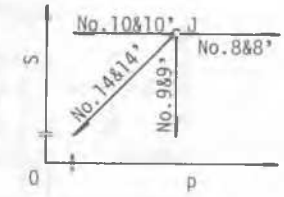

Fig.5 Stress probes of series 2 and 3

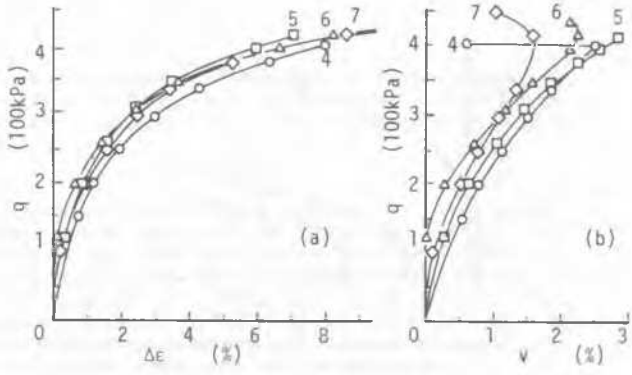

Fig.4 (a) Shear strain and (b) volumetric strain in first half of axial compression (series 1)

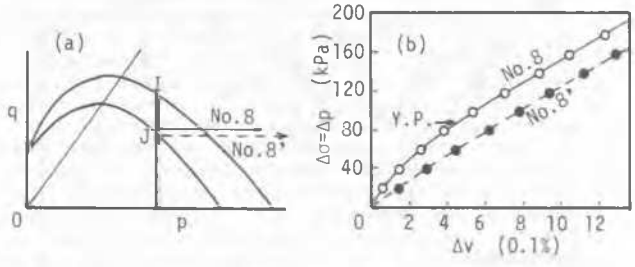

Fig.6 (a) Difference in yield loci
(b) Decision of yield stress of No.8

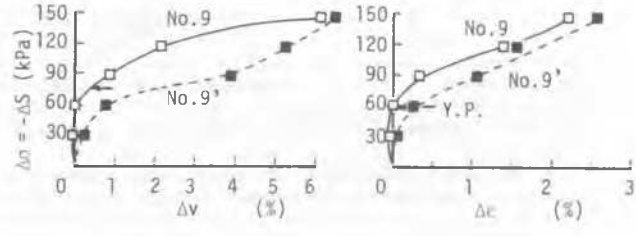

Fig.7 Decision of yield stresses of No.9

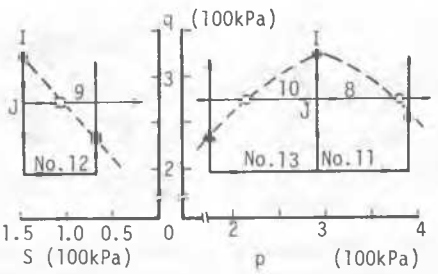

Fig.8 Stress paths and yield points of series 4

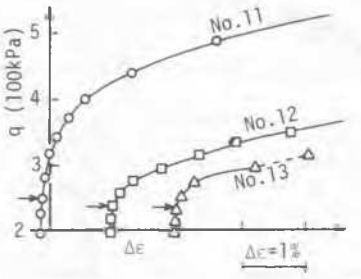

Fig.9 Decision of yield stresses of series 4

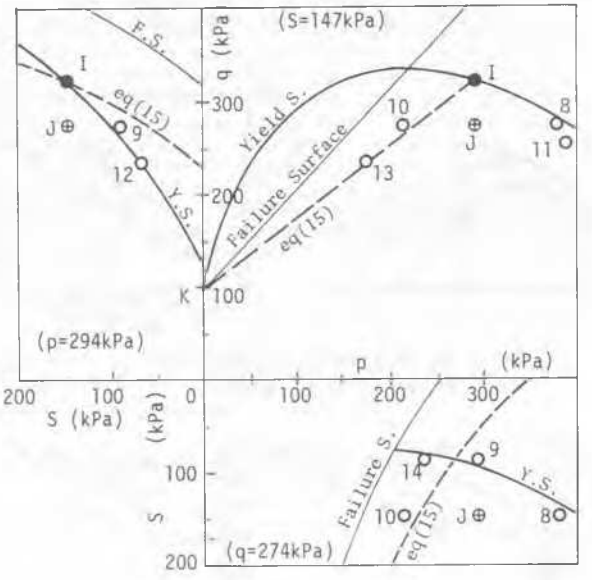

Fig.10 Distribution of observed yield points and theoretical yield loci (b=0)

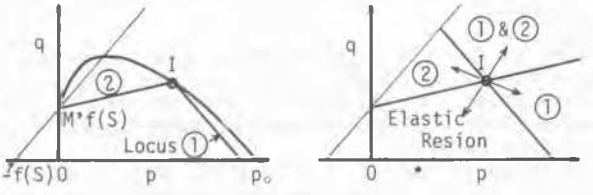

Fig.11 (a) Combined yield loci and (b) their applications

to q-direction. Because a sharp bending point appeared on curve as seen in Fig.9, that point was regarded as a yield point. Yield points were also obtained from No.12 and No.13. In Fig.10 all yield points are shown with the section of theoretical yield surface. It is seen that No.8,9,11,12 and 14 are located close to theoretical surface. However there is no corresponding surface to yield points of No.10 and 13.

DISCUSSIONS AND CONCLUSIONS

Distribution of yield points No.10 and 13 implies existence of another yield surface like dotted lines in Fig.10, of which equations is

$$q = M' f(S) + \frac{q_1 - M' f(S_1)}{p_1} p \qquad (15)$$

where, suffix 1 means the components of stress point I.
Therefore combined potential functions of plastic strains increments are introduced, which consist of a surface sloping (-M') to p-axis through point I and eq(15) shown as ① and ② in Fig.11. Strain increments are given as follows,

$$\begin{cases} dv_1^p = \dfrac{dv^p}{1 - [\dfrac{q - M' f(S)}{M' p}]} & (16) \\ d\varepsilon_1 = \dfrac{1}{M}, dv_1^p & (17) \end{cases}$$

$$\begin{cases} dv_2^p = -[\dfrac{q - M' f(S)}{M' p}]^2 dv_1^p & (18) \\ d\varepsilon_2 = -[\dfrac{p}{q - M' f(S)}]^2 dv_2^p & (19) \end{cases}$$

where $(dv^p{}_1, d\varepsilon_1)$ and $(dv^p{}_2, d\varepsilon_2)$ are the strains increments associated with locus ① and ②, respectively.

REFERENCES

Alonso,E.E., Gens,A., and Hight,D. (1987). General Report for Session 5, Preprint of 9th European Conf. SMFE.

Barden,L., Maddor,A.O. and Widger,R.A. (1969). Proc. ASCE, Vol.95, SM1, pp.33-51.

Coleman,D.J. (1962). Geotechnique, Vol.12, 4, pp.384-350.

Fledlund,D.G., Morgenstern,N.R. and Widger,R.A. (1978). Canadian Geotechnical Journal, Vol.15, No.3, pp.313-321.

Jennings,J.E. and Burland,J.B. (1962). Geotechnique, Vol.12, No.2, pp.125-144.

Karube.D., Kato.S., and Katsuyama.J. (1986). Proc. JSCE, No.376/III-5, pp.179-188.

Karube.D. (1986). ASTM, STP977. pp. 539-552.

Karube.D. (1987a). Proc. Symp. on Unsaturated Soils, Osaka, Japan, pp.59-68.

Karube.D. (1987b). Proc. 7ARC-SMFE, pp.33-35.

Katsuyama.J., Nishiuni.N. and Karube.D. (1987). Proc. Annual Conf., JSCE,3, pp.148.

Kogo.Y. (1987). Proc. Symp. on Unsaturated SoilS, Osaka, Japan, pp.69-77.